Nucleic Acids Research, 2006, Vol. 34, No. 5 ***1369–1380***
doi:10.1093/nar/gkl001

In situ fluorescence analysis demonstrates active siRNA exclusion from the nucleus by Exportin 5

Thomas Ohrt, Dennis Merkle, Karin Birkenfeld, Christophe J. Echeverri[1] and Petra Schwille*

Institute for Biophysics, BIOTEC, Dresden University of Technology, Tatzberg 47-51, 01307 Dresden, Germany and [1]Cenix BioScience GmbH, Tatzberg 47, 01307 Dresden, Germany

Received December 14, 2005; Revised and Accepted February 9, 2006

ABSTRACT

Two types of short double-stranded RNA molecules, namely microRNAs (miRNAs) and short interfering RNAs (siRNAs), have emerged recently as important regulators of gene expression. Although these molecules show similar sizes and structural features, the mechanisms of action underlying their respective target silencing activities appear to differ: siRNAs act primarily through mRNA degradation, whereas most miRNAs appear to act primarily through translational inhibition. Our understanding of how these overlapping pathways are differentially regulated within the cell remains incomplete. In the present work, quantitative fluorescence microscopy was used to study how siRNAs are processed within human cells. We found that siRNAs are excluded from non-nucleolar areas of the nucleus in an Exportin-5 dependent process that specifically recognizes key structural features shared by these and other small RNAs such as miRNAs. We further established that the Exportin-5-based exclusion of siRNAs from the nucleus can, when Exp5 itself is inhibited, become a rate-limiting step for siRNA-induced silencing activity. Exportin 5 therefore represents a key point of intersection between the siRNA and miRNA pathways, and, as such, is of fundamental importance for the design and interpretation of RNA interference experimentation.

INTRODUCTION

Argonaute-containing complexes are emerging as key regulators of gene expression, both in the context of controlling developmental programs of gene expression and as a defence mechanism to protect the genome against viruses and transposons [Reviewed in (1–3)]. These complexes have been shown to use short double-stranded RNA (dsRNA) molecules as targeting co-factors, to identify cognate mRNA transcripts whose expression is to be silenced. The mechanism by which this silencing occurs is also determined in part by the type of dsRNA molecule used, and two mechanisms have emerged, directed by two distinct types of short dsRNA: small interfering RNAs (siRNAs) and micro RNAs (miRNAs).

Documented in organisms from plants to humans, siRNAs are key intermediates of an evolutionarily conserved, multistep pathway for post-transcriptional gene silencing known as RNA interference (RNAi) (4–6). This process occurs in the cytoplasm and is guided by the siRNAs which direct the sequence-specific degradation of targeted mRNAs (7–9). Naturally occurring siRNAs are produced by Dicer-based processing of long dsRNA molecules derived from viral infection or transposon activity (10–12). These siRNAs consist of a dsRNA stem of ~19 nt containing 2 nt overhangs with free hydroxyl groups at both 3′ ends and phosphates at both 5′ ends (6). To act as triggers for mRNA degradation, siRNAs are assembled with specific proteins including Argonaute 2 to form the RNA-induced silencing complex (RISC), which catalyzes target mRNA cleavage (7,13–15). The siRNA strand with the most thermodynamically labile base pairing near its 5' end is preferentially used by RISC as the ''guide'' or targeting strand, whereas the other ''passenger'' strand is degraded (16,17). The target cleavage site in the mRNA is defined by the siRNA sequence and is located 10 nt upstream of the nucleotide complementary to the 5′-most residue of the guide strand (18,19).

miRNAs represent a similar yet clearly distinct class of short RNA species, as these are actually encoded by animal and viral genomes to direct the post-transcriptional silencing of target genes, also using RISC-like complexes (20–23). With hundreds of such molecules having now been identified in various organisms, miRNAs emerge as 21–25 nt-long single-stranded hairpin RNAs, derived from larger precursors that form imperfect stem–loop structures and in most cases, inhibit translation from target mRNAs in a process that remains poorly understood (24). Two processing events lead to mature miRNA formation, as well as to their specific

*To whom correspondence should be addressed. Tel: +49 351 463 40328; Fax: +49 351 463 40342; Email: petra.schwille@biotec.tu-dresden.de

subcellular localization in animals. The nascent miRNA transcript (pri-miRNA) is processed by the RNase-III enzyme Drosha inside the nucleus into an ~70 nt precursor (pre-miRNA) (25). Pre-miRNAs are then exported from the nucleus into the cytoplasm by Exportin-5 (Exp5), a Ran-GTP dependent nucleo–cytoplasmic transporter (26). Once the pre-miRNA has entered the cytoplasm it is further processed by the RNase-III enzyme Dicer to form the mature miRNA (27,28).

Fundamentally, siRNAs and miRNAs share some common characteristics, e.g. the dsRNA stem, the Dicer dependent maturation (8,27,28) and the association with Argonaute-family proteins to direct their gene silencing activity (14,29–31). It has been shown in *Drosophila* that miRNAs and siRNAs are incorporated into different, but similar effector complexes, where miRNAs associate with AGO1 and siRNAs with AGO2 as key components of RISC (29,30). The degree of complementarity between a siRNA or miRNA and their target mRNA determines, at least in part, the specific mode of post-transcriptional repression. That is, fully complementary short RNAs lead to the degradation of the target mRNA, whereas multiple mismatches in the RNA:mRNA helix direct translational repression without destabilization of the mRNA (32).

The detailed analysis of siRNA and miRNA processing is of fundamental interest to better understand their respective pathways and to further refine the experimental power of RNAi techniques. In the present work we employed high-resolution fluorescence microscopy to quantitatively measure fluorescence-labelled siRNAs delivered into HeLa SS6 cells by microinjection. We examined the cellular localization of a variety of siRNA-like structures, which yielded new insight into how siRNA molecules are processed in cells. These observations led to the demonstration that Exp5 is required for the active exclusion of siRNAs from the nucleus and thereby directly impacts their biological activity. This study reveals Exp5-mediated nuclear export as another important step common to the processing of both naturally encoded miRNAs and exogenous synthetic siRNAs, and as such, one that must be taken into careful consideration during RNAi experimentation.

MATERIALS AND METHODS

Cell culture

Adherent HeLa SS6 cells were cultured at 37°C in DMEM (Gibco, Invitrogen GmbH) with 10% fetal calf serum (PAA Laboratories GmbH). Cells were regularly passaged at subconfluency and were plated in antibiotic-free medium with 2–3.5 × 10^4 cells/ml density.

For all transfections cells were transfected with Lipofectamine 2000 (Invitrogen GmbH). For the luciferase assays exponentially growing cells were trypsinized on the day before transfection and plated into 24-well plates at a density of 5 × 10^4 cells/well in antibiotic-free media. For 6-well plates and MatTek chambers (MatTek Corporation, USA) cells were sown one day before transfection at a density of 1.5–3 × 10^5 cells/well in antibiotic-free media. The next day, the cells were transfected with 100 nM siRNAs with 6 µl Lipofectamine 2000 and 300 µl OptiMEM in 1.5 ml fresh medium. The medium is replaced by 2 ml fresh growth medium 3–5 h after transfection.

siRNAs

RNA and DNA oligonucleotides were obtained from IBA GmbH (Goettingen) and Ambion. For the silencing of CRM1, Exp5, Pp-luc and the following oligonucleotides were used:

g = guide strand; p = passenger strand

siCRM1: p UGUGGUGAAUUGCUUAUACTT; g GUAUAAGCAAUUCACCACATT

siExp5-1: p GCCCUCAAGUUUUGUGAGGTT; g CCUCACAAAACUUGAGGGCTT

siExp5-2: p UGUGAGGAGGCAUGCUUGUTT; g ACAAGCAUGCCUCCUCACATT

siGL2: p CGUACGCGGAAUACUUCGATT; g UCGAAGUAUUCCGCGUACGTT

siEGFP: p GCAGCACGACUUCUUCAAGTT; g CUUGAAGAAGUCGUGCUGCTT.

As negative controls a negative siRNA (NegsiRNA) from Ambion was used and DNAs were obtained from IBA GmbH.

DNA-GL2: p CGTACGCGGAATACTTCGATT; g TCGAAGTATTCCGCGTACGTT

NegsiRNA: *Silencer*™ Negative Control #1 siRNA.

For the 3′–5′ overhang shift assay

siGL2: g UCG AAG UAU UCC GCG UAC GUG

siGL2: 3′2ntoh/-3′: p CGU ACG CGG AAU ACU UCG AUU

siGL2: blunt/-3′: p CAC GUA CGC GGA AUA CUU CGA

siGL2: 5′2ntOh: p AUC ACG UAC GCG GAA UAC UUC

siGL2: 5′4ntOh: p ACA UCA CGU ACG CGG AAU ACU

siGL2: 5′5ntOh: p AAC AUC ACG UAC GCG GAA UAC

siGL2: 5′6ntOh: p GAA CAU CAC GUA CGC GGA AUA

siGL2: 3′4ntOh: p GUA AAG CUU CAU AAG GCG CAU

siGL2: 3′5ntOh: p UGU AAA GCU UCA UAA GGC GCA

siGL2: 3′6ntOh: p CUG UAA AGC UUC AUA AGG CGC

Duplex siRNAs were prepared by mixing complementary sense siRNA and antisense siRNA at equimolar ratio, incubating at 80°C for 2 min followed by a cooling step at 1°C/min to 15°C. The annealing procedure was performed in the Mastercycler epGradientS (Eppendorf) in 110 mM K-gluconate; 18 mM NaCl; 10 mM HEPES, pH 7.4 and 0.6 mM $MgSO_4$ with 10–60 µM siRNA concentrations. The quality of the duplex siRNAs was checked by agarose gel electrophoresis and high-performance liquid chromatography. The prepared siRNA duplexes were stored at −20°C.

Fluorescence-reporter plasmids

pEGFP-N1 vector (Clontech) and pDsRed2-N1 vector (Clontech).

Agarose gel electrophoresis

For agarose gel electrophoresis a special high resolving Metaphor® agarose (Cambrex) was used. All agarose gels have a 4% (w/v) concentration and were used with 1× TBE (0.1 M Tris–borate, 2 mM EDTA, pH 8.3) running buffer. Aliquots of 1 × 10^{-2} nmol labelled siRNA were loaded in each pocket. The gels were analysed with a Typhoon 9410 Variable Mode Imager (Amersham Biosciences) by using the

manufacturer's settings for Alexa488 (Molecular Probes) and Cy5 (Amersham Biosciences).

Labelling

RNA and DNA oligonucleotides were synthesized by IBA with a 3′ or 5′-amino group via a C6-carbon linker and were labelled with Alexa Fluor® 488 carboxylic acid, 2,3,5,6-tetrafluorophenyl ester (Alexa488-TFP; Molecular Probes) or Cy5 succinimidyl ester (Cy5-NHS; Amersham Biosciences).

Single-stranded oligonucleotides (0.2 μmol) in 55 μl H_2O were mixed in 20 μl of 500 mM borate buffer, pH 8.5, with 25 μl of 10 mM aminoreactive dye [in *N*,*N*-dimethylformamide, Merck] and incubated at room temperature for 16 h. Labelled siRNAs were ethanol precipitated [70% (v/v) ethanol, 250 mM NaOAc, pH 5.8] four times to remove most of the free unreacted dye. The pre-purified siRNAs were loaded on an 18% denaturating polyacrylamide gel (SequaGel® Sequencing system; National diagnostics) to separate unlabelled and labelled strands and unreacted dye. The band with the labelled RNA is cut out and eluted from the gel slice with 400 μl of 0.3 M NaCl for 12 h at 4°C. To remove residual gel the sample was loaded onto a microfilter with 0.2 μm^2 pore size (Nanosep® MF, PALL).

Luciferase assay

Dual-luciferase assays (Promega GmbH) were performed 24–48 h after transfection according to the manufacturer's protocol for 24-well chambers and detected with a TD20/20 luminometer (Turner designs). *Pp*-luc target vector (pGL2-Control, Promega) was co-transfected with the control vector Rr-luc (pRL-TK; Promega GmbH).

Lipofectamine 2000 (Invitrogen GmbH) was used for the triple transfection of the dual luciferase assay vectors pGL2-control [contains the cDNA of Firefly luciferase (FL)] and pRL-TK [contains the cDNA of Renilla luciferase (RL)] together with the siRNAs. The desired amount of each siRNAs was mixed with 0.9 μg pGL2-control and 0.1 μg pRL-TK. To circumvent any non-specific effects caused by different nucleic acid content, all transfections were performed at equal final nucleic acid concentrations as indicated in the figures and figure legends. For this adjustment we used a short double-stranded DNA (dsDNA) (Eg5). The cells were transfected with the indicated amounts of siRNAs, 100 μl Opti-MEM and 2 μl Lipofectamine 2000. The medium was replaced by 500 μl fresh growth medium 3–5 h after transfection.

Microinjection

For microinjection, 1.2×10^5 HeLa SS6 cells were transfered onto MatTek chambers coated with poly-D-lysine (0.1 mg/ml; Sigma) 24 h before microinjection. The micropipette (Femtotip 2; Eppendorf) was loaded with 20 μM labelled siRNAs in 110 mM K-gluconate; 18 mM NaCl; 10 mM HEPES, pH 7.4 and 0.6 mM $MgSO_4$. The micromanipulator consists of a FemtoJet and InjectMan NI2 which was mounted directly on an Olympus microscope IX-71. Working pressure for injection in adherent cells was between 45–90 hPa for 0.1 s and a holding pressure of 35–40 hPa. For the injection of plasmids the injection pressure was kept below 90 hPa to avoid destructive shearing.

Laser scanning confocal fluorescence microscopy

LSM imaging was performed using a commercial Zeiss ConfoCor 2 laser scanning microscope (Zeiss, Jena, Germany) with argon ion (488 nm, 25 mW, at 18% of maximum power output), helium–neon (543, 1 mW, at 30% of maximum power output) and helium–neon (633 nm, 5.0 mW, at 12% of maximum power) lasers. A water immersion objective 40×/1.2W (Zeiss) was used in the epidetection configuration with an adjustable pinhole set at 71 μm. A band-pass filter transmitting 505–550 nm (Zeiss) was used in the experiments with Alexa488, while a long-pass filter at 650 nm (Zeiss) was applied to separate Cy-5 fluorescence. For the experiments with DsRed2 and EGFP a water immersion objective 20×/0.5W Ph2 (Zeiss) was used in the epidetection configuration with an adjustable pinhole set at 73.4 μm for the red channel and 80 μm for the green channel. A band-pass filter transmitting 505–530 nm (Zeiss) was used in the experiments with EGFP, while a long-pass filter at 560 nm (Zeiss) was applied to separate DsRed2 fluorescence. In order to avoid saturation of the fluorescence intensity in the scanned images the detector settings were optimized by using the feature Range Indicator provided by the Zeiss software (Operating Manual LSM510; Zeiss, Jena, Germany).

Cell extract and western blot

For western blot analysis the cells were lysed 48 h after siRNA transfection (100 nM or siRNA amounts are indicated in the figure) with PLC buffer [1% (v/v) TX100; 10% (v/v) glycerol; 150 mM NaCl; 50 mM HEPES, pH 7.4; 1.5 mM $MgCl_2$; 1 mM EGTA; 0.2 mM PMSF; 0.1 μg/ml Pepstatin; 0.1 mM Benzamide] for 15 min at 4°C. The crude extracts were sonicated 10 times (Bandelin, Sonopuls; duration, 0.1 sec; power, 10%) and centrifuged 10 min at 14 000 r.p.m. (Eppendorf 5417R). The supernatant was frozen in liquid nitrogen and stored at −80°C. The S20 HeLa extract was prepared as described by Ford and Wilusz (33) except that the final centrifugation step was performed at 20 000 *g* instead of 100 000 *g*.

For immunoblotting, proteins were run on an 8% PAGE and subsequently transferred onto Protran® Nitrocellulose Transfer Membrane (Schleicher & Schuell) by semi-dry blotting. Membranes were blocked for 1 h in phosphate-buffered saline (PBS) containing 5% milk and 0.05% Tween (PBS-T), incubated for 1 h with a primary antibody, followed by a 1 h incubation of the secondary antibody linked to horseradish peroxidase (Novagen). Immunoreactive protein bands were detected using ECL™ western blotting detection reagents according to the manufacturer's protocol (Amersham Biosciences) and a documentary station (LAS 3000, Fujifilm).

Antibodies

CRM1 (Santa Cruz): H-300; Dilution 1:600 (rabbit, polyclonal)

GAPDH-HRP (Abcam): Clone mAbcam 9484; Dilution 1:40000 (mouse monoclonal)

Alpha-Tubulin (Sigma): Clone DM1A; Dilution 1:100000 (mouse, monoclonal)

Exportin-5 [kindly provided by U. Kutay (26)]: Dilution 1:1000 (rabbit, polyclonal)

Anti-rabbit-HRP(Dianova): Dilution 1:40000 (goat)

Anti-mouse-HRP (Dianova): Dilution 1:40000 (goat).

RESULTS

Establishment of labelling and delivery conditions for *in situ* study of siRNA processing

Single strands of a pre-validated siRNA sequence directed against Firefly luciferase (siGL2) (5) were synthesized and subsequently fluorescently labelled on the 3′ and 5′ ends with Alexa488 on the guide strand and Cy5 on the passenger strand (Figure 1A and B). These single-stranded RNAs (ssRNAs) were also purified from a polyacrylamide gel and subsequently annealed to produce the active siGL2 dsRNA (Materials and Methods and Figure 1B). To examine if the 3′ linked dyes had any influence on silencing, the double-labelled siGL2 dsRNA was co-transfected with the reporter plasmid combination pGL2-Control/ pRL-TK-Control into HeLa SS6 cells (5). Luciferase activities were determined 48 h after transfection by a dual luciferase assay (Figure 1C) and the ratios of target to control luciferase were normalized to a NegsiRNA, which has no significant sequence similarity to mouse, rat or human gene sequences. For comparison, the interference ratios of the siGL2 labelled variants were grouped together for each concentration. Both unlabelled (Figure 1C, grey bars) and double 3′ labelled (Figure 1C, open bars) duplexes showed a similar concentration-dependent silencing of Firefly luciferase, consistent with previous studies in which various 3′ modifications were examined (34,35). Furthermore, using an siRNA against Renilla luciferase (siTK) and switching Alexa488 to the passenger strand and Cy5 to the guide strand also did not change the silencing activity of the siRNA (data not shown). A 5′ dual-labelled siGL2 (Figure 1A) was also tested in this system, since it has been shown that blocking of the 5′ end of the guide strand has a strong

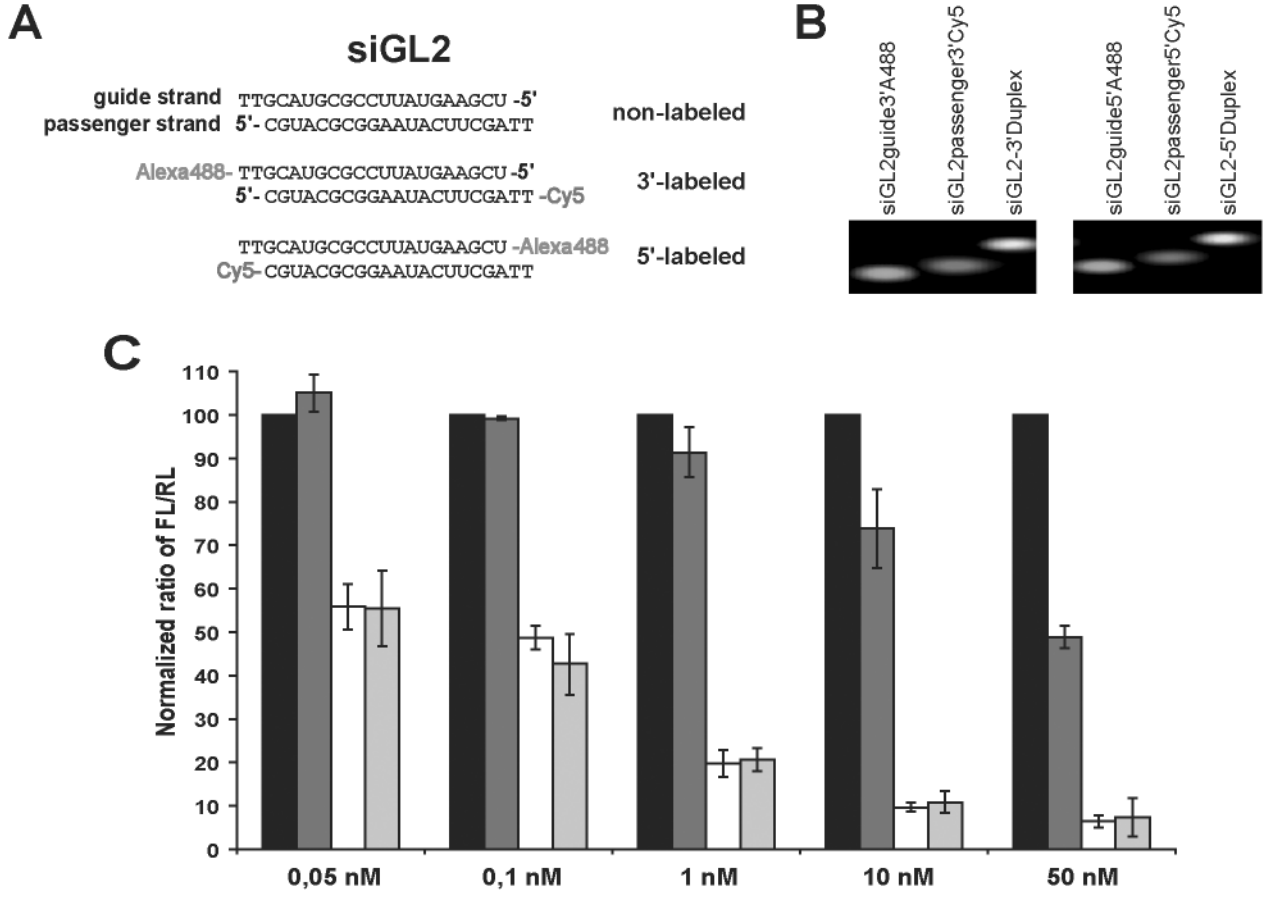

Figure 1. Effect of 3′ and 5′ dual labelling on siRNA activity. (**A**) Illustration of differently labelled GL2 siRNA (siGL2) with Alexa488 and Cy5 used for targeting firefly luciferase (pGL2-control). (**B**) Purification control of the labelled siRNAs (as described in Materials and Methods) on a 4% agarose gel. In the left panel the guide strand, 3′ labelled with Alexa488, indicated as siGL2guide3′A488 and the passenger strand, 3′ labelled with Cy5, indicated as siGL2passenger3′Cy5 are shown. The annealed double 3′ labelled siGL2 duplex (siGL2-3′-Duplex) is shown in lane 3. The 5′ labelled variants of siGL2 are shown in the right panel, starting with the guide strand labelled with Alexa488 (siGL2guide5′A488), followed by the passenger strand labelled with Cy5 (siGL2passenger5′Cy5). The annealed 5′ double-labelled siGL2 duplex (siGL2-5′-Duplex) is shown in lane 3. (**C**) HeLa SS6 cells were transfected with the indicated amounts of differently labelled siGL2 together with the fixed concentration of the pGL2-Control [Firefly luciferase (FL)] and pRL-TK [Renilla luciferase (RL)] reporter plasmids as described in Materials and Methods. After 48 h the ratios of target to control luciferase concentration were normalized to the NegsiRNA control indicated in black; the 5′ double-labelled siGL2 is indicated by the dark grey bar; the 3′ double-labelled siGL2 is indicated by the open bar; the unlabelled siGL2 is indicated by the grey bar. The plotted data were averaged from six independent experiments ±SD.

deleterious impact on siRNA silencing activity (7,34). The 5′ labelled siGL2 showed no significant silencing activity up to 1 nM and could not silence firefly luciferase beyond 50% even at 50 nM concentrations (Figure 1C, dark grey bar). These results demonstrate that siRNAs dual labelled with Alexa488 and Cy5 on the 3′ termini have no detectible impact on silencing activity and are therefore a suitable dye pair for *in situ* observations. Additionally, it was confirmed that blocking of the 5′ end of the guide strand is inhibitory towards efficient RNAi (7,34,35).

Labelled siRNAs were microinjected directly into the cytoplasm in order to monitor their subcellular location. This was done to avoid potential risks of siRNA segregation within endocytic compartments, as can occur with lipid-based transfection methods. To confirm that microinjected siRNAs participate in the RNAi pathway, we developed a dual fluorescent reporter system to quantify target-silencing efficiency. The reporter plasmids pEGFP-N1 (expressing EGFP protein) and pDsRed2-N1 (expressing DsRed2 protein) were co-microinjected into HeLa SS6 cells together with either an unlabelled siRNA targeting EGFP (siEGFP) or the unlabelled NegsiRNA with no target (described above). After 48h the cells were imaged by laser scanning confocal microscopy (Figure 2A), and all red cells were further analysed. The ratio of green-expressing cells to red-expressing cells was calculated (Figure 2B). In three independent injection experiments, fluorescent cells from the negative control (NegsiRNA) injections exhibited a ratio of ~1.0, indicating that the expression levels of both DsRed2 and EGFP were not differentially affected by NegsiRNA (Figure 2A, left panel; Figure 2B, closed symbols). When the reporter plasmids were injected together with siEGFP (Figure 2A, right panel; Figure 2B, open symbols), the ratio of green to red cells decreased with increasing amounts of siEGFP. This result demonstrated that siRNAs delivered directly to the cytoplasm via microinjection successfully entered the RNAi pathway and mediated sequence-specific silencing.

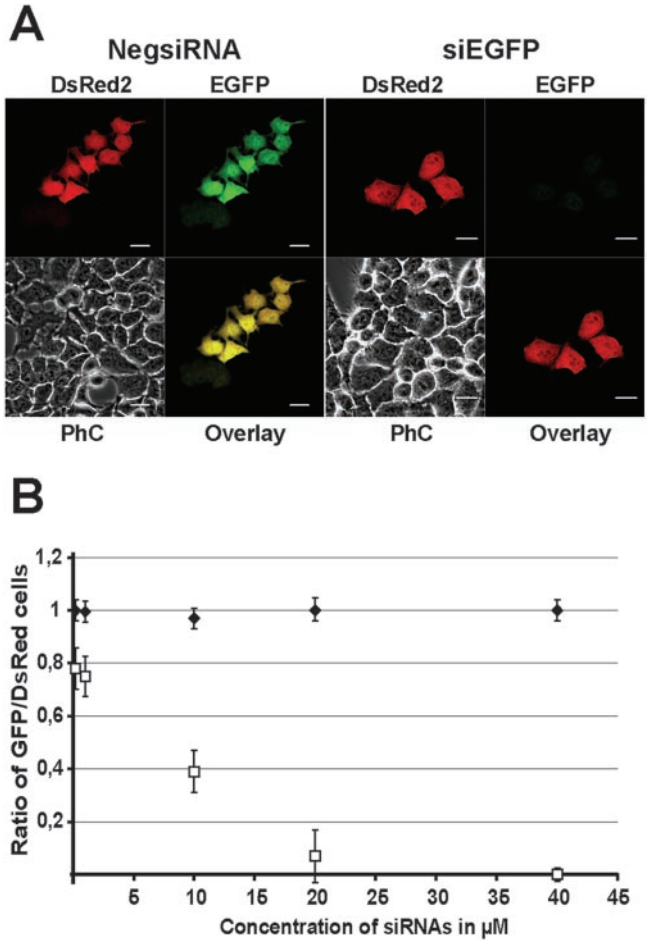

Figure 2. Dual fluorescence-reporter assay for silencing activity analysis of microinjected siRNAs. (**A**) HeLa SS6 cells were microinjected with 2.5 ng/µl of both pDsRed2-N1 and pEGFP (Ratio 1:1) together with NegsiRNA panel 1 or siEGFP directed against EGFP panel 2. Recording of the confocal pictures was after 48 h. Scale bars = 20 µm. (**B**) Quantitative analysis of silencing after microinjection with the indicated siRNA concentrations. To normalize the results the number of red and green cells is divided by the total number of counted cells (in each experiment >50 cells). NegsiRNA effect on DsRed2 and EGFP expression is shown in closed symbol (closed diamond), siEGFP in open symbols (open square). The plotted data were averaged from three independent experiments ±SD.

siRNAs are specifically excluded from non-nucleolar regions of the nucleus

We investigated the impact of several key determinants of siRNA structure on the subcellular localization of labelled siRNA-like molecules after microinjection into the cytoplasm of cultured human cells. We prepared single-labelled siRNAs (siGL2) as well as labelled controls consisting of ssRNAs (siGL2-ssRNA), dsDNAs (siGL2-DNA) of the same size and single-stranded DNAs (siGL2-ssDNA) of the same size (Materials and Methods). These variants were then microinjected at a concentration of 20 µM into the cytoplasm of HeLa SS6 cells. An intra-needle siRNA concentration of 20 µM was found to give effective silencing activity (Figure 2B) as well as detectible fluorescence signal intensities under our recording conditions (Figure 3). The intracellular concentration of microinjected siRNAs, as measured by fluorescence correlation spectroscopy (FCS), was ~250 nM (data not shown).

Within 15 min after microinjection, the labelled siGL2 was located predominantly throughout the cytoplasm. The siRNA was excluded from the nucleus, with the exception of faint fluorescence in the nucleolar region. Although the nucleolar fluorescene increased over time (open arrow), the siRNA was excluded from non-nucleolar regions of the nucleus for >1 h post-injection, irrespective of which siRNA strand was labelled ((Figure 3A and data not shown). After 1 h, the fluorescence intensity increased slightly in the non-nucleolar regions of the nucleus, which could be due to degradation of the labelled siRNAs (Figure 3A). No difference was observed when labelling with Alexa488 (Figure 3B, left panel) or Cy5 (Figure 3D, left panel). Similar results were obtained with other siRNA sequences targeting endogenous genes (such as the kinesin-related motor protein Eg5), and with a different cell line (HEK cells; data not shown). In contrast to the results obtained with siGL2 dsRNA, microinjection of labelled siGL2-ssRNA yielded a marked accumulation of fluorescence signal within all areas of the nucleus regardless of the dye used (Figure 3B and D, right panel) or the end that was labelled (Figure 3F, left panel). This result

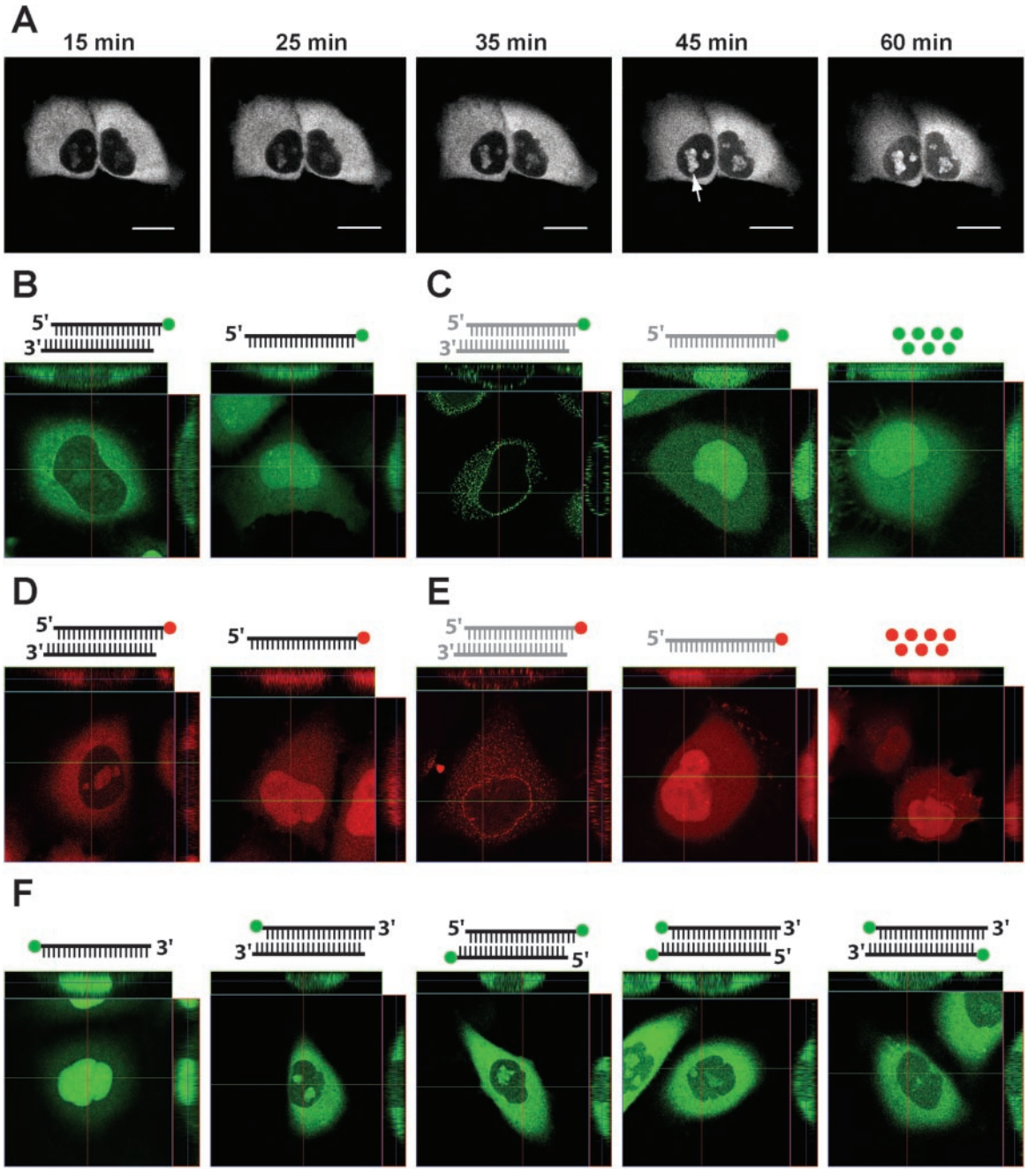

Figure 3. Subcellular localizations of different types of nucleic acids after microinjection into the cytoplasm. HeLa SS6 cells were cultured in 35 mm dishes with glass cover slip bottoms. Graphical representations of double-stranded and single-stranded nucleic acids are indicated above the confocal images and the fluorescence dye is indicated as coloured circle (green indicates Alexa488 and red indicates Cy5). RNA is indicated by the black and DNA by the grey backbone in the illustration. Localization of the nucleic acids was monitored by confocal microscopy. The confocal images represent a single plane through the cell and the cross sections of the stack of the cell are indicated by the lines and illustrated on top and to the right of each image, respectively. (**A**) Time course of nuclear exclusion of siGL2 labelled with Alexa488 on the 3′ end. The time after microinjection is indicated above the images. Nucleoli localization is indicated by an arrow at 45 min. Scale bars = 20 μm. (**B**) Subcellular localization of siGL2 labelled on the 3′ end of the guide strand with Alexa488 in HeLa SS6 cells (left panel) and of the labelled siGL2-ssRNA (guide strand, right panel). (**C**) As controls siGL2-dsDNA were used labelled on the 3′ end strand with Alexa488 as well as siGL2-ssDNA alone and free Alexa488 dye. (**D**) Subcellular localization of siGL2 labelled on the 3′ end of the guide strand with Cy5 (left panel) and the siGL2-ssRNA in the right panel. (**E**) As controls siGL2-dsDNA was used labelled on the 3′ end with Cy5 as well as the labelled siGL2-ssDNA and free Cy5 dye. (**F**) Subcellular localization of differently single- and double-labelled siGL2-dsRNA with Alexa488 on both 3′ or 5′ or either 3′ and 5′ ends in HeLa SS6 cells.

indicated that the strandedness of the RNA was important for the observed exclusion from the nucleus.

In order to determine whether the type of nucleic acid backbone is important for the observed localization, we examined labelled dsDNAs and ssDNAs of equivalent sizes. As seen in Figure 3 for ssRNA, injection of siGL2-ssDNA showed fluorescence signals accumulating throughout the nucleus, whereas the siGL2-dsDNA showed

a punctate, non-homogeneous distribution in the cytoplasm. The stability of these various strands in S20 HeLa extracts was not significantly altered, suggesting that the subcellular localizations observed after microinjection of labelled double-stranded nucleic acids were not degradation artefacts (Supplementary data). In addition, free dye also showed marked accumulation in the nucleus (Figure 3C and E, right panel). These results demonstrated that the double-stranded nature of the siRNA, as well as the ribose backbone structure, were required for both the observed nuclear exclusion and nucleolar accumulation (Figures 3D, right panel and Figure 3E).

Previous RNAi studies showed an influence of the 3′ and 5′ overhangs of siRNAs on silencing activity (18,36). We therefore investigated whether 3′ or 5′ end structures were also necessary for nuclear exclusion. First, to determine whether free ends are needed, we tested siRNAs dually labelled on both 3′ or 5′ termini, or juxtaposed 3′ and 5′ termini. Dual labelling always resulted in the nuclear exclusion of the siRNA (Figure 3F, right panels). Next, we examined the effects of shifting the siRNA's passenger strand towards the 3′ or 5′ end of the guide strand, thus producing progressively longer or shorter symmetric 5′ or 3′ overhangs, respectively (Figure 4A). The quality of all annealed dsRNA preparations was verified by agarose gel electrophoresis, which confirmed both the absence of ssRNA contamination and the expected shifts in duplex mobility corresponding to the progressive lengthening of the overhanging ends (Figure 4B). These different siRNA-like variants were then microinjected into HeLa SS6 cells and analysed after 10–15 min by confocal microscopy. The resulting ratios of nuclear to cytoplasmic staining intensities were quantified by taking mean fluorescence intensity measurements from three 20 μm^2 regions within the nucleus and the cytoplasm of injected cells. In Figure 4C, these nuclear to cytoplasmic fluorescence intensity ratios are shown for each siRNA-like variant, with clear

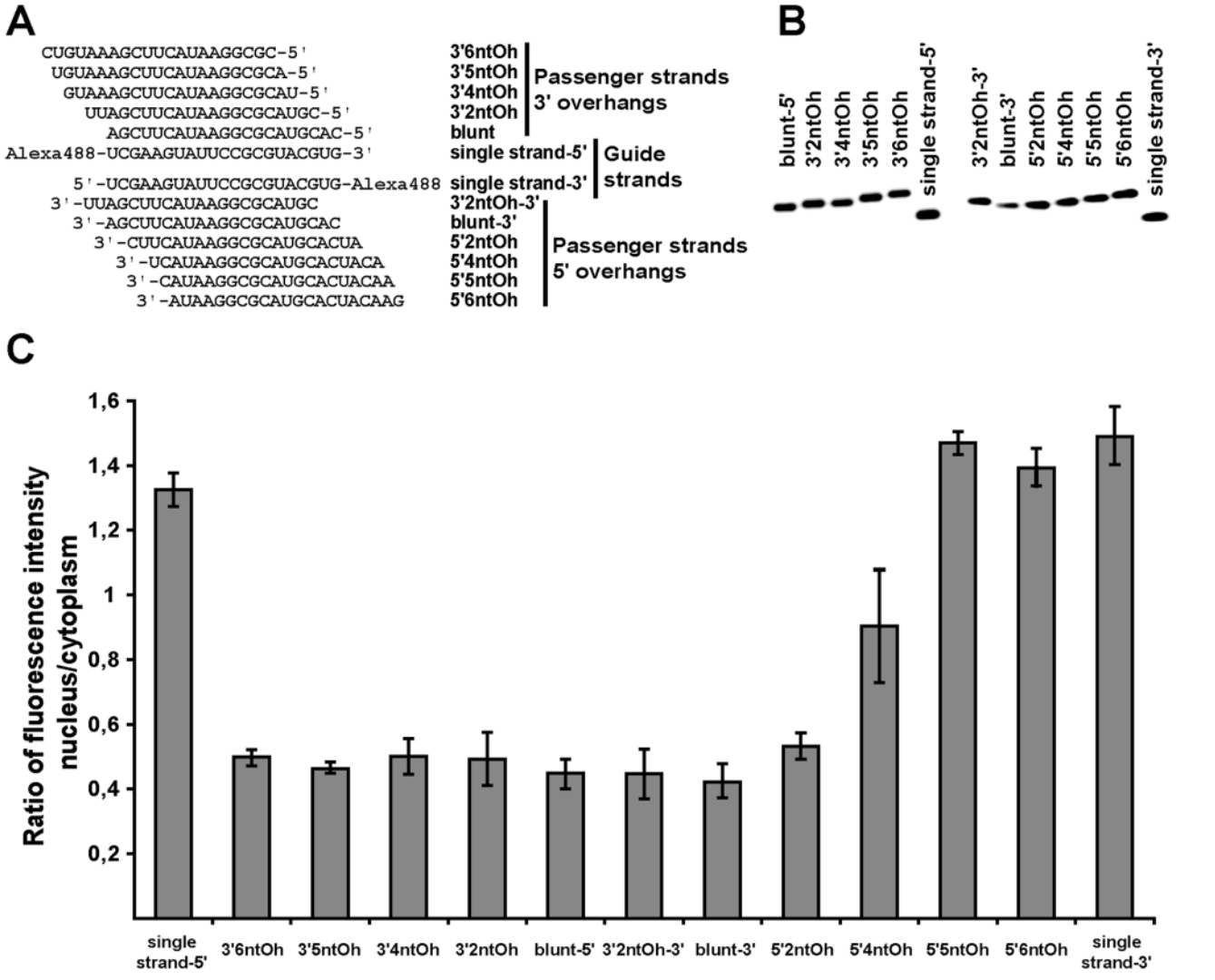

Figure 4. Influence of different 3′ and 5′ overhangs on the subcellular localization of short dsRNAs. (**A**) Sequences and their annealing pattern of the different shifted siGL2 variants were illustrated together with their used abbreviations. For the comparison of the 3′ and the 5′ overhangs two labelled strands were used to keep the dye close to the double-stranded stem. (**B**) Quality control of the shifted GL2 short RNAs for non-annealed single strands as described in Materials and Methods with a 4% agarose gel. (**C**) Each type of short RNA labelled with Alexa488 was microinjected into HeLa SS6 cells and analysed 10–15 min later with confocal microscopy. The graph shows the ratio of fluorescence intensity nucleus/cytoplasm.

nuclear exclusion corresponding to values smaller than 0.6. Such nuclear exclusion was observed with siRNA-like variants that were either blunt-ended, that contained 5′ overhangs of up to 2 nt, or 3′ overhangs of up to 6 nt (Figure 4C). The siRNA with a 5′ overhang of 4 nt (5′4ntOh) showed a slight nuclear exclusion initially, but also resulted in marked accumulation in the nucleus (Figure 4C). All siRNA-like variants containing longer 5′ overhangs (5′5ntOh, 5′6ntOh) immediately accumulated in the nucleus (Figure 4C), as seen with ssRNA. The dsRNA variants that were excluded from the nucleus showed a consistent nuclear to cytoplasmic ratio of 0.45–0.55 (Figure 4C). Conversely, the 5′4ntOh duplex showed a value around 0.9 while the samples containing 5′5ntOh, 5′6ntOh and ssRNA showed values around 1.4 (Figure 4C). Nuclear to cytoplasmic ratios were confirmed by FCS-based concentration measurements of the various constructs in the nucleus and cytoplasm (data not shown). These results indicate that while overhanging ends are not necessary for nuclear exclusion of siRNA-like molecules, this localization pattern is not detectably affected by 3′ overhangs of up to 6 nt and is strongly inhibited by the presence of 5′ overhangs of more than 2 nt.

siRNAs, like pre-miRNAs are exported from the nucleus by Exportin-5

Our observed nuclear exclusion of siRNAs, as well as its associated structural determinants, are reminiscent of those reported previously for certain naturally occurring short dsRNAs including pre-miRNAs (37,38), which have been shown previously to be exported from the nucleus by the Ran-GTP dependent nucleo/cytoplasmic transporter, Exportin-5 (Exp5) (26,39,40). We therefore tested whether Exp5-based nuclear export activity was also required for our observed nuclear exclusion of siRNAs.

To this end, we examined the effects of Exp5 knockdown on the nuclear exclusion of siRNAs, as well as their silencing activity. As a control to monitor the specificity of any observed Exp5 knockdown phenotypes, we also silenced the export receptor CRM1, which is unable to transport small, structured, minihelix-containing RNAs (26). Furthermore, we also used two distinct, previously validated siRNAs targeting Exp5 (siExp5-1 and siExp5-2) and CRM1 (siCRM1) (26), all of which yielded effective silencing in our experiments, as confirmed by immunoblotting of the corresponding proteins (Figure 5A). To quantify and normalize the result, we developed a two-colour fluorescence assay consisting of 3′ Cy5 labelled siGL2 and 3′ labelled Alexa488 5′5ntOh (Figure 4A). These duplexes displayed opposite subcellular localizations, as the Cy5 labelled siGL2 was excluded from the nucleus whereas the 5′5ntOh variant accumulated throughout the nucleus (Figure 4). Knockdown of CRM1 had no detectable effect on the subcellular localizations of either siGL2 or 5′5ntOh (Figure 5B, left panel) compared with Figure 4C. In contrast, when Exp5 was knocked down with either siExp5-1 or siExp5-2, siGL2 was found to accumulate together with 5′5ntOh within all areas of the nucleus, with perhaps some slight exclusion from nucleoli (Figure 5B, right panel).

In order to precisely measure this effect of Exp5 knockdown, we quantified mean fluorescence intensities for each reporter molecule (siGL2 in red and 5′5ntOh in green) from three 20 μm^2 sampling areas taken in the cytoplasm and in the nucleus, thus generating normalized, concentration-independent siGL2 and 5′5ntOh nuclear to cytoplasmic ratios. For the CRM1 knock down, the nuclear to cytoplasmic ratio of the siGL2 was around 0.55, whereas the ratio of 5′5ntOh was ~1.2, reflecting the preferential nuclear exclusion of siGL2 but not of 5′5ntOh (Figure 5C). After Exp5 knock down the ratio of siGL2 displayed a ratio of ~3.5, which means approximately six times higher concentration inside the nucleus compared with non treated cells or CRM1 (Figures 4 and 5). This high ratio also indicates a 2.5-fold stronger accumulation of the siGL2 duplexes for the nucleus in contrast to the 5′5ntOh ratio of 1.2–1.4 in Exp5 knocked down cells. Additionally, the nuclear/cytoplasmic ratio of 5′5ntOh in each knockdown experiment always resulted in values around 1.2–1.4 (Figure 5C), which is consistent with the characterization observed in Figure 4. These results show that Exp5 activity is responsible for the nuclear exclusion of siRNAs observed in our experiments and does not detectibly affect the localization of the 5′5ntOh variant.

Exp5-based nuclear exclusion is a key determinant of siRNA silencing efficacy

To test whether the Exp5-dependent exclusion of siRNAs from the nucleus represents a contributing factor towards the efficacy of siRNA-driven target silencing in these cells, we knocked down Exp5 for 48 h and then measured siRNA silencing using a dual luciferase assay (Figure 6A). Importantly, for this portion of the study, all siRNAs were delivered using standard lipid-based transfection, thus enabling whole population analyses and also serving as additional confirmation of microinjection-based observations under conditions typically used for RNAi experimentation. To control for the specificity of any observed Exp5 knockdown phenotypes, siExp5-1 and siExp5-2 (data not shown), as well as NegsiRNA were all used at the same concentrations in parallel experiments. The NegsiRNA was then also used as a specificity control for siGL2 silencing in the subsequent luciferase assays. As expected, both types of negative control samples (NegsiRNA/NegsiRNA and siExp5/NegsiRNA) showed similar FL/RL ratios at all concentrations tested. All positive control samples pre-treated with the control NegsiRNA and transfected with siGL2, yielded strong and specific silencing of the targeted FL, as reflected by a FL/RL ratio of ~25%. Cells pre-treated with low concentrations of Exp5-targeting siRNAs (1 and 10 nM) (yielding ~98% and ~50% of control Exp5 protein levels, respectively) gave similar results. However, the knock down of Exp5 at 100 nM siRNA concentration brought Exp5 protein down to 15% of its control level (that is an 85% knock down of Exp5) and did exhibit a clearly detectible increase in FL/RL ratio to 55% (Figure 6B and C). Under these experimental conditions, this result reflects an ~2-fold reduction in siGL2 silencing efficacy that is directly attributable to Exp5 knockdown. These results also confirm the importance of Exp5-mediated export for the siRNA silencing effects shown in Figures 3–5, and is independent of the siRNA delivery method (i.e. microinjection independent) used in those experiments.

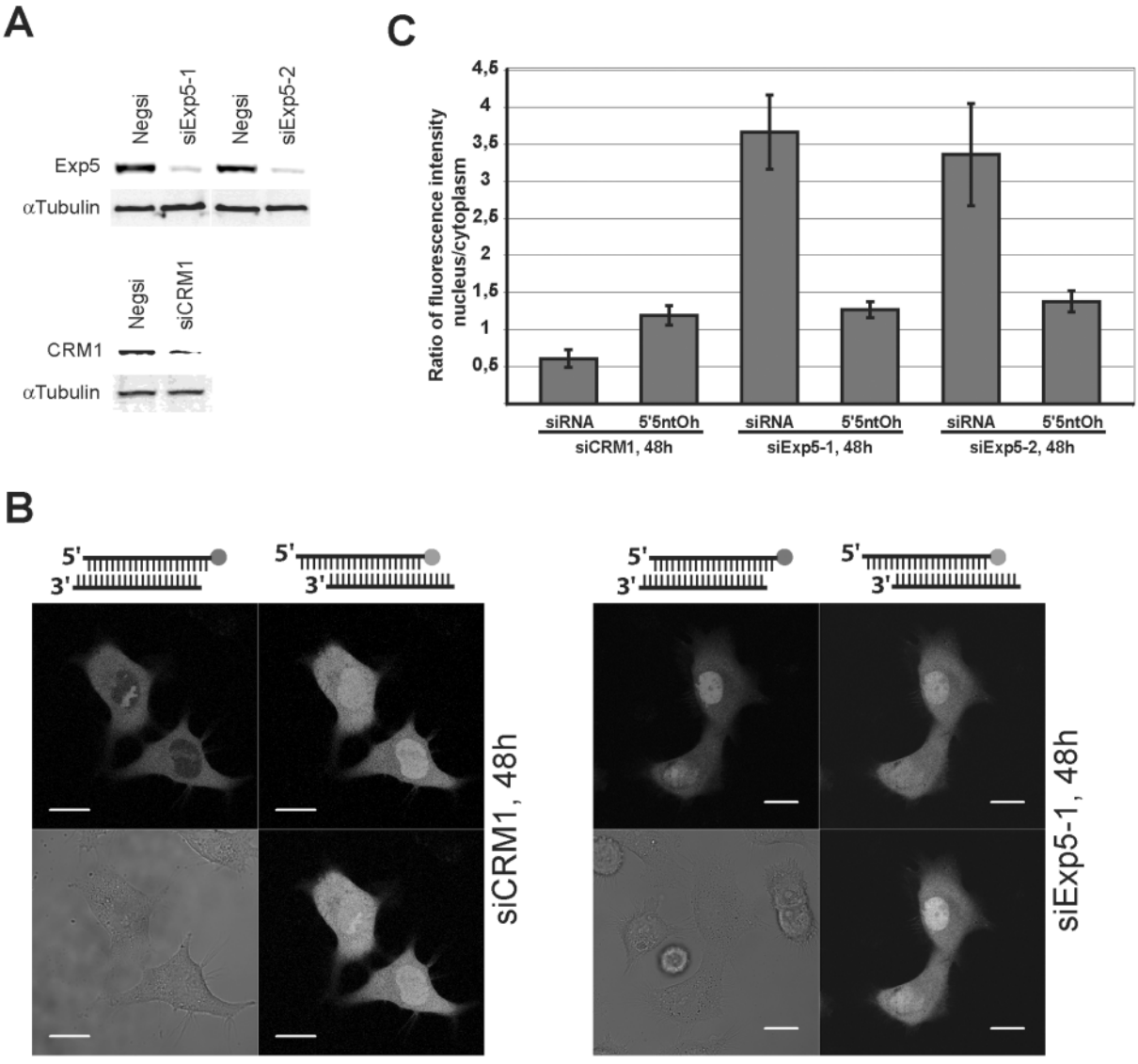

Figure 5. Exportin-5 is responsible for the exclusion of siRNAs from the nucleus. (**A**) After 48 h total protein extracts from CRM1, siExp5-1 and siExp5-2 (100 nM) transfected cells were immunoblotted with antibodies against Exp5 and CRM1. α-Tubulin was used as a loading control. (**B**) HeLa SS6 cells were transfected with siCRM1 (left panel), siExp5-1 (right panel) or siExp5-2 (data not shown) and were microinjected 48 h later with a mixture consisting of 20 μM 3′2ntOh (Figure 4A) labelled with Cy5 and 20 μM 5′5ntOh (Figure 4A) short dsRNA labelled with Alexa488. The cells were analysed 10–15 min after microinjection by laser scanning microscopy. Scale bars = 20 μm. (**C**) Quantification of the translocation process. The confocal images were analysed by using fluorescence area intensity measurements in the nucleus and in the cytoplasm for the two RNA duplexes. The graph shows the ratio of fluorescence intensity nucleus/cytoplasm.

DISCUSSION

With the goal of better understanding how cells differentially use and process siRNA and miRNA molecules, we first established fluorescence labelling conditions that would enable intracellular detection of biologically active siRNAs in living cells by confocal microscopy, FCS and LSM. Consistent with previous reports (7,34,35), we found this to be possible only with fluorescent labels conjugated to either or both 3′ ends, whereas 5′ labels were found to significantly diminish siRNA silencing. Standard lipid-based (5) or peptide-based (41) transfection protocols often produce variable results with respect to probe localization. Therefore, to study the intracellular distribution of labelled siRNAs in living cells, we injected labelled siRNAs directly into the cytosol. With this approach, the RNAs successfully entered the RNAi pathway, mediated sequence-specific target mRNA silencing, and provided consistent and clearly interpretable intracellular fluorescence patterns *in situ*.

These patterns revealed a near-total exclusion of labelled siRNAs from non-nucleolar areas of the nucleus, restricting them to a homogeneous cytosolic distribution accompanied by a marked accumulation within nucleoli. Although the latter observation has been noted in previous studies (41), its physiological relevance remains unclear. The same cytosolic pattern was observed with all injected siRNAs, irrespective of whether or not they had an endogenous mRNA target present. Even at low concentrations, the cytosolic siRNA distribution did not exhibit any detectible foci such as those noted by others who observed a co-localization of miRNAs and

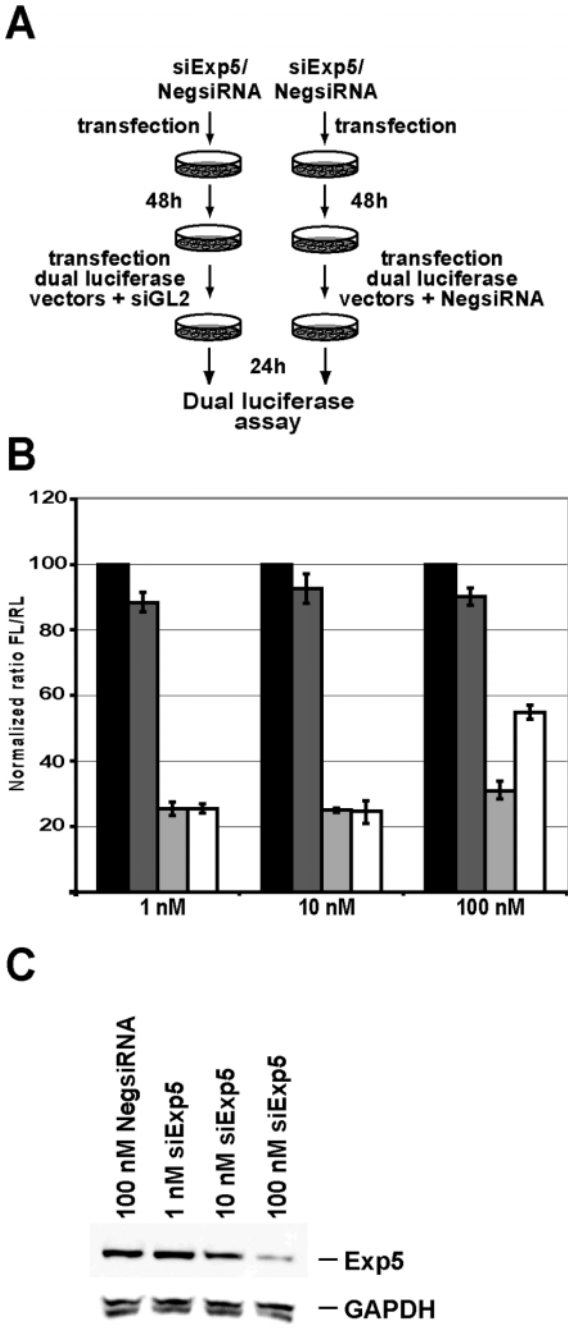

Figure 6. Exportin-5 knockdown leads to reduced silencing efficiency. (**A**) An outline of the experiment is illustrated. First the cells were transfected with different amounts of siExp5-1 and NegsiRNA and were incubated for 48 h. Then the cells were transfected with the dual luciferase reporter plasmids pGL2-Control (Firefly luciferase) and pRL-TK (Renilla luciferase) together with 1 nM siGL2 or NegsiRNA as a control for 24 h. (**B**) Dual luciferase results were obtained 24 h after transfection of the pGL2-Control (Firefly luciferase) and pRL-TK (Renilla luciferase) reporter plasmids together either with siGL2 or the NegsiRNA. Results were grouped together for each siRNA concentration used for 48 h. The ratios of target to control luciferase were normalized to the NegsiRNA control transfected for 48 h and for the luciferase assay indicated in black. The transfection of first the NegsiRNA for 48 h followed by siGL2 is shown in light grey, whereas the siExp5-1 transfection for 48 h followed by NegsiRNA is shown in dark grey and the siExp5-1 followed by siGL2 in white. (**C**) After 48 h total protein extracts from siExp5-1 transfected cells were immunoblotted with antibodies against Exp5 and GAPDH-HRP was used as a loading control. The plotted data were averaged from four independent experiments ±SD.

imperfectly-targeting siRNA-like molecules with cognate target mRNAs within so-called processing bodies (42). While such foci could conceivably have been masked by the relatively high concentrations of labelled siRNAs in our experiments, it also remains possible that siRNAs which mediate silencing through perfect matching to their target mRNAs do not accumulate long enough—or at all—at these sites, otherwise known to be involved in mRNA degradation. This issue is now being further investigated.

The nuclear exclusion proved to be specific to siRNA-like molecules, which contrasted with ssRNA and ssDNA molecules of equivalent nucleotide length, or even unconjugated dyes, all of which accumulated evenly throughout the cytosol and nucleus. Interestingly, dsDNA strongly accumulated in punctuate cytoplasmic foci and at the nuclear envelope, though the relevance of this pattern, if any, remains unclear. The observed siRNA distribution was thus reminiscent of that reported by others for certain naturally occurring short dsRNA molecules, such as adenoviral VA1 RNA and pre-miRNAs (37,38). During miRNA maturation, pre-miRNAs are exported from the nucleus by Exp5 (26,39,40). The recognition of pre-miRNA by Exp5 is dependent upon characteristics of the pre-miRNA structure (38,43,44) such as a double-stranded stem of at least 14 nt with either blunt ends, 3′ overhangs up to 6 nt, or 5′ overhangs up to 2 nt. Consistent with this, we observed that our own siRNA-like constructs containing either blunt ends or 3′ overhangs of up to 6 nt were successfully excluded from the nucleus, while those with 5′ overhangs >2 nt were not. This led us to hypothesize that siRNAs, like pre-miRNAs, are subjected to an active process of Exp5-based exclusion from non-nucleolar areas of the nucleus. This was supported by our finding that the observed nuclear exclusion of siRNAs is strongly attenuated by silencing of Exp5. Furthermore, our finding that several siRNA molecules containing completely distinct sequences were all similarly excluded from the nucleus indicates that the apparent cytosolic destination signal is sequence independent. This signal, consistent with the mini-helix motif serving as an export signal (37), thus appears to be strictly comprised of those structural characteristics shared by all siRNAs and pre-miRNAs, and found herein to be recognized for nuclear export by Exp5 (38,43).

As we quantified the effects of Exp5 knockdown on the siRNA-directed silencing efficiency in cells, we observed an ∼2-fold reduction in silencing of Firefly luciferase upon knockdown of Exp5, compared with a NegsiRNA control. This result is contradictory to the findings by Yi *et al.* (40,45) who found no effect on silencing after Exp5 knock down. This is likely due to key differences between experimental conditions used in the two studies. In particular, Yi *et al.* (40,45) employed the same siRNA against firefly luciferase at a concentration of 100 nM, whereas we used 1 nM, thereby making our readout more sensitive in this case. The level of siGL2 used by Yi *et al.* (40,45) may have been high enough to saturate all compartments of the cell, thereby compensating for the reduced Exp5 activity and effectively masking its role in RNAi silencing in those experiments. Indeed, under our own experimental conditions, the dual luciferase assay showed similar results as those observed by Yi *et al.* (40,45), when applied at 100 nM siGL2 after Exp5 knock down (data not shown). We therefore conclude that, under conditions of low siRNA concentrations

often used in standard lipofection-based RNAi experimentation, the level of Exp5 expression and/or activity in the chosen cells can represent a rate-limiting factor for target silencing.

Since Exp5 activity also represents a key step in the processing of endogenous miRNAs, these observations also warrant the question of whether RNAi experimentation, as typically carried out in many laboratories today, may in fact interfere with endogenous miRNA functions. Interestingly, Yi *et al*. (45) demonstrated that the overexpression of artificial short hairpin RNAs (shRNAs) can inhibit the biological activity of endogenous miRNAs, and that this inhibition can be rescued by Exp5 overexpression. The resulting conclusion that endogenous Exp5 activity may represent a limiting step in the miRNA pathway, especially when the cell is 'flooded' with high concentrations of exogenous shRNA molecules, is now extended by our present findings linking Exp5 activity to siRNA silencing. It is therefore likely that transfected siRNAs can also compete with endogenously transcribed pre-miRNAs for binding to Exp5 and hence affect miRNA function in cells. While miRNA targeting remains poorly understood, it is widely believed that most endogenous miRNAs function as high level 'managers' of gene expression programs, contributing to the maintenance of differentiated cell states by controlling the levels of large groups of genes at the same time (2,24). As such, endogenous miRNA deregulation by siRNA 'flooding' of Exp5 represents a potential source for at least some of the complex and unpredictable off-target effects that have been linked to the use of excessively high concentrations of RNAi silencing reagents (46,47). It has even been shown that the deregulation of some miRNAs is associated with certain types of cancers (48), thus further highlighting the risk that such artefacts could significantly alter the basic physiology of cells during RNAi experiments. Importantly, as there is no evidence to date supporting any dependence of such an Exp5 flooding effect on the specific sequences of the siRNAs, this type of off-target effect remains easily controlled for by the use of samples transfected with equivalent concentrations of 'scrambled' or 'unspecific' siRNAs, such as the NegsiRNA used in the present study.

Because of the fact that siRNAs accumulate ~2.5 times stronger in the nucleus after Exp5 knockdown compared with shifted siRNAs, ssRNA, dsDNA, ssDNA and free dye, this potentially indicates binding to nuclear structures or complexes of the siRNAs. If siRNAs aberrantly accumulate in the nucleus, then should we worry about off-target effects there? Two recent reports have shown specific and potent RNAi mechanisms in the nucleus (49 ,50). We showed that siRNAs can shuttle between the cytoplasm and the nucleus, mediated by diffusion into the nucleus and export out of the nucleus in a RanGTP/Exp5-dependent fashion. A remnant nuclear dislocation of a fraction of the siRNA duplexes, at high concentrations, was confirmed by LSM and FCS. Furthermore, it has also been shown that siRNAs can induce transcriptional gene silencing in human cells through a mechanism that involves DNA methylation [RNA-directed DNA methylation (RdDM)], an RNAi-related process, that has been shown to occur in the nucleus and affect gene function at the level of genomic DNA (51,52). Both the effects of nuclear RNAi and RdDM were dominant at high concentrations and only if the dsRNAs predominantly entered the nucleoplasm. This influx of dsRNA molecules into the nucleus may also result in (non)-specific consequences on gene expression since nuclear dsRNAs can cause the activation of non-cytoplasmic RNAi pathways. Previous studies in *Caenorhabditis elegans* have shown that the expression of retrotransposons increases when genes implicated in dsRNA-mediated silencing are mutated (53). This supports the idea that a nuclear RNAi machinery may be used to regulate retrotransposon expression in humans too. These types of silencing or phenotype effects, if they occur at all, may or may not be sequence dependent. The use of shRNAs and stabilized siRNAs should be taken under careful consideration and must be validated by multiple scrambled sequences.

In addition to these commonly used controls, our findings further highlight the value of using well-validated RNAi silencing reagents at their lowest effective concentrations to minimize the risks of artefacts arising from 'flooding' of key steps common to both the siRNA and miRNA pathways, as well as cytoplasmic RNAi-related mechanisms. Future *in situ* analyses of RNA–protein interactions should help to further elucidate other common or distinct processes underlying these pathways.

SUPPLEMENTARY DATA

Supplementary Data is available at NAR Online.

ACKNOWLEDGEMENTS

We are grateful to Dr Ulrike Kutay for anti-Exp5 antibody. We thank Drs Anthony Hyman and Martin Srayko for helpful comments on this manuscript. We also thank members of the Schwille laboratory, especially Wolfgang Staroske for the FCS measurements, Drs Nicoletta Kahya and Elke Haustein for critical discussions as well as Anne Grabner (Cenix BioScience GmbH) for suggestions and criticisms of this manuscript. This work was supported by the DFG (SPP 1128). Funding to pay the Open Access publication charges for this article was provided by the DFG (SPP 1128).

Conflict of interest statement. None declared.

REFERENCES

1. Meister,G. and Tuschl,T. (2004) Mechanisms of gene silencing by double-stranded RNA. *Nature*, **431**, 343–349.
2. Ambros,V. (2004) The functions of animal microRNAs. *Nature*, **431**, 350–355.
3. He,L. and Hannon,G.J. (2004) MicroRNAs: small RNAs with a big role in gene regulation. *Nature Rev. Genet*., **5**, 522–531.
4. Fire,A., Xu,S., Montgomery,M.K., Kostas,S.A., Driver,S.E. and Mello,C.C. (1998) Potent and specific genetic interference by double-stranded RNA in *Caenorhabditis elegans*. *Nature*, **391**, 806–811.
5. Elbashir,S.M., Harborth,J., Lendeckel,W., Yalcin,A., Weber,K. and Tuschl,T. (2001) Duplexes of 21-nucleotide RNAs mediate RNA interference in cultured mammalian cells. *Nature*, **411**, 494–498.
6. Elbashir,S.M., Lendeckel,W. and Tuschl,T. (2001) RNA interference is mediated by 21- and 22-nucleotide RNAs. *Genes Dev*., **15**, 188–200.
7. Nykänen,A., Haley,B. and Zamore,P.D. (2001) ATP requirements and small interfering RNA structure in the RNA interference pathway. *Cell*, **107**, 309–321.
8. Bernstein,E., Caudy,A.A., Hammond,S.M. and Hannon,G.J. (2001) Role for a bidentate ribonuclease in the ignition step of RNA interference. *Nature*, **409**, 363–366.

9. Zeng,Y. and Cullen,B.R. (2002) RNA is restricted to the cytoplasm. *RNA*, **8**, 855–860.
10. Billy,E., Brondani,V., Zhang,H., Muller,U. and Filipowicz,W. (2001) Specific interference with gene expression induced by long, double-stranded RNA in mouse embryonal teratocarcinoma cell lines. *Proc. Natl Acad. Sci. USA*, **98**, 14428–14433.
11. Zhang,H., Kolb,F.A., Brondani,V., Billy,E. and Filipowicz,W. (2002) Human Dicer preferentially cleaves dsRNAs at their termini without a requirement for ATP. *EMBO J.*, **21**, 5875–5885.
12. Provost,P., Dishart,D., Doucet,J., Frendewey,D., Samuelsson,B. and Rådmark,O. (2002) Ribonuclease activity and RNA binding of recombinant human Dicer. *EMBO J.*, **21**, 5864–5874.
13. Hammond,S.M., Bernstein,E., Beach,D. and Hannon,G.J. (2000) An RNA-directed nuclease mediates post-transcriptional gene silencing in *Drosophila* cells. *Nature*, **404**, 293–296.
14. Hammond,S.M., Boettcher,S., Caudy,A.A., Kobayashi,R. and Hannon,G.J. (2001) Argonaute2, a link between genetic and biochemical analyses of RNAi. *Science*, **293**, 1146–1150.
15. Martinez,J., Patkaniowska,A., Urlaub,H., Lührmann,R. and Tuschl,T. (2002) Single-stranded antisense siRNAs guide target RNA cleavage in RNAi. *Cell*, **110**, 563–574.
16. Schwarz,D.S., Hutvàgner,G., Du,T., Xu,Z., Aronin,N. and Zamore,P.D. (2003) Asymmetry in the assembly of the RNAi enzyme complex. *Cell*, **115**, 199–208.
17. Tomari,Y., Matranga,C., Haley,B., Martinez,N. and Zamore,P.D. (2004) A protein sensor for siRNA asymmetry. *Science*, **306**, 1377–1380.
18. Elbashir,S.M., Martinez,J., Patkaniowska,A., Lendeckel,W. and Tuschl,T. (2001) Functional anatomy of siRNAs for mediating efficient RNAi in *Drosophila melanogaster* embryo lysate. *EMBO J.*, **20**, 6877–6888.
19. Martinez,J. and Tuschl,T. (2004) RISC is a 5′ phosphomonoester-producing RNA endonuclease. *Genes Dev.*, **18**, 975–980.
20. Lee,R.C., Feinbaum,R.L. and Ambros,V. (1993) The *C.elegans* heterochronic gene lin-4 encodes small RNAs with antisense complementarity to lin-14. *Cell*, **75**, 843–854.
21. Reinhart,B.J., Slack,F.J., Basson,M., Pasquinelli,A.E., Bettinger,J.C., Rougvie,A.E., Horvitz,H.R. and Ruvkun,G. (2000) The 21-nucleotide let-7 RNA regulates developmental timing in *Caenorhabditis elegans*. *Nature*, **403**, 901–906.
22. Ambros,V., Lee,R.C., Lavanway,A., Williams,P.T. and Jewell,D. (2003) MicroRNAs and other tiny endogenous RNAs in *C.elegans*. *Curr. Biol.*, **13**, 807–818.
23. Pfeffer,S., Zavolan,M., Grasser,F.A., Chien,M., Russo,J.J., Ju,J., John,B., Enright,A.J., Marks,D., Sander,C. *et al.* (2004) Identification of virus-encoded microRNAs. *Science*, **304**, 734–736.
24. Bartel,D.P. (2004) MicroRNAs: Genomics, biogenesis, mechanism, and function. *Cell*, **116**, 281–297.
25. Lee,Y., Ahn,C., Han,J., Choi,H., Kim,J., Yim,J., Lee,J., Provost,P., Radmark,O., Kim,S. *et al.* (2003) The nuclear RNase III Drosha initiates microRNA processing. *Nature*, **425**, 415–419.
26. Lund,E., Guttinger,S., Calado,A., Dahlberg,J.E. and Kutay,U. (2004) Nuclear export of microRNA precursors. *Science*, **303**, 95–98.
27. Hutvagner,G., McLachlan,J., Pasquinelli,A.E., Balint,E., Tuschl,T. and Zamore,P.D. (2001) A cellular function for the RNA-interference enzyme Dicer in the maturation of the let-7 small temporal RNA. *Science*, **293**, 834–838.
28. Lee,Y., Jeon,K., Lee,J., Kim,S. and Kim,V.N. (2002) MicroRNA maturation: stepwise processing and sub-cellular localization. *EMBO J.*, **21**, 4663–4670.
29. Caudy,A.A., Myers,M., Hannon,G.J. and Hammond,S.M. (2002) Fragile X-related protein and VIG associate with the RNA interference machinery. *Genes Dev.*, **16**, 2491–2496.
30. Okamura,K., Ishizuka,A., Siomi,H. and Siomi,M.C. (2004) Distinct roles for Argonaute proteins in small RNA-directed RNA cleavage pathways. *Genes Dev.*, **18**, 1655–1666.
31. Meister,G., Landthaler,M., Patkaniowska,A., Dorsett,Y., Teng,G. and Tuschl,T. (2004) Human Argonaute2 mediates RNA cleavage targeted by miRNAs and siRNAs. *Mol. Cell*, **15**, 185–197.
32. Doench,J.G., Petersen,C.P. and Sharp,P.A. (2003) siRNAs can function as miRNAs. *Genes Dev.*, **17**, 438–442.
33. Ford,L.P. and Wilusz,J. (1999) An *in vitro* system using HeLa cytoplasmic extracts that reproduces regulated mRNA stability. *Methods*, **17**, 21–27.
34. Chiu,Y.L. and Rana,T.M. (2002) RNAi in human cells: Basic structural and functional features of small interfering RNA. *Mol. Cell*, **10**, 549–561.
35. Harborth,J., Elbashir,S.M., Vandenburgh,K., Manninga,H., Scaringe,S.A., Weber,K. and Tuschl,T. (2003) Sequence, chemical, and structural variation of small interfering RNAs and short hairpin RNAs and the effect on mammalian gene silencing. *Antisense Nucleic Acid Drug Dev.*, **13**, 83–105.
36. Czauderna,F., Fechtner,M., Dames,S., Aygun,H., Klippel,A., Pronk,G.J., Giese,K. and Kaufmann,J. (2003) Structural variations and stabilising modifications of synthetic siRNAs in mammalian cells. *Nucleic Acids Res.*, **31**, 2705–2716.
37. Gwizdek,C., Bertrand,E., Dargemont,C., Lefebvre,J.C., Blanchard,J.M., Singer,R.H. and Doglio,A. (2001) Terminal minihelix, a novel RNA motif that directs polymerase III transcripts to the cell cytoplasm. Terminal minihelix and RNA export. *J. Biol. Chem.*, **276**, 25910–25918.
38. Zeng,Y. and Cullen,B.R. (2004) Structural requirements for pre-microRNA binding and nuclear export by Exportin 5. *Nucleic Acids Res.*, **32**, 4776–4785.
39. Brownawell,A.M. and Macara,I.G. (2002) Exportin-5, a novel karyopherin, mediates nuclear export of double-stranded RNA binding proteins. *J. Cell Biol.*, **156**, 53–64.
40. Yi,R., Qin,Y., Macara,I.G. and Cullen,B.R. (2003) Exportin-5 mediates the nuclear export of pre-microRNAs and short hairpin RNAs. *Genes Dev.*, **17**, 3011–3016.
41. Chiu,Y.L., Ali,A., Chu,C.Y., Cao,H. and Rana,T.M. (2004) Visualizing a correlation between siRNA localization, cellular uptake, and RNAi in living cells. *Chem. Biol.*, **11**, 1165–1175.
42. Pillai,R.S., Bhattacharyya,S.N., Artus,C.G., Zoller,T., Cougot,N., Basyuk,E., Bertrand,E. and Filipowicz,W. (2005) Inhibition of translational initiation by Let-7 MicroRNA in human cells. *Science*, **309**, 1573–1576.
43. Gwizdek,C., Ossareh-Nazari,B., Brownawell,A.M., Doglio,A., Bertrand,E., Macara,I.G. and Dargemont,C. (2003) Exportin-5 mediates nuclear export of minihelix-containing RNAs. *J. Biol. Chem.*, **278**, 5505–5508.
44. Gwizdek,C., Ossareh-Nazari,B., Brownawell,A.M., Evers,S., Macara,I.G. and Dargemont,C. (2004) Minihelix-containing RNAs mediate exportin-5-dependent nuclear export of the double-stranded RNA-binding protein ILF3. *J. Biol. Chem.*, **279**, 884–891.
45. Yi,R., Doehle,B.P., Qin,Y., Macara,I.G. and Cullen,B.R. (2005) Overexpression of Exportin 5 enhances RNA interference mediated by short hairpin RNAs and microRNAs. *RNA*, **11**, 220–226.
46. Semizarov,D., Frost,L., Sarthy,A., Kroeger,P., Halbert,D.N. and Fesik,S.W. (2003) Specificity of short interfering RNA determined through gene expression signatures. *Proc. Natl Acad. Sci. USA*, **100**, 6347–6352.
47. Jackson,A.L., Bartz,S.R., Schelter,J., Kobayashi,S.V., Burchard,J., Mao,M., Li,B., Cavet,G. and Linsley,P.S. (2003) Expression profiling reveals off-target gene regulation by RNAi. *Nat. Biotechnol.*, **21**, 635–637.
48. Gregory,R.I. and Shiekhattar,R. (2005) MicroRNA biogenesis and cancer. *Cancer Res.*, **65**, 3509–3512.
49. Robb,G.B., Brown,K.M., Khurana,J. and Rana,T.M. (2005) Specific and potent RNAi in the nucleus of human cells. *Nature Struct. Mol. Biol.*, **12**, 133–137.
50. Langlois,M.A., Boniface,C., Wang,G., Alluin,J., Salvaterra,P.M., Puymirat,J., Rossi,J.J. and Lee,N.S. (2005) Cytoplasmic and nuclear retained DMPK mRNAs are targets for RNA interference in Myotonic Dystrophy cells. *J. Biol. Chem.*, **280**, 16949–16954.
51. Morris,K.V., Chan,S.W., L, Jacobsen,S.E. and Looney,D.J. (2004) Small interfering RNA-induced transcriptional gene silencing in human cells. *Science*, **305**, 1289–1292.
52. Matzke,M.A. and Birchler,J.A. (2005) RNAi-mediated pathways in the nucleus. *Nature Rev. Genet.*, **6**, 24–35.
53. Ketting,R.F., Haverkamp,T.H., van Luenen,H.G. and Plasterk,R.H. (1999) Mut-7 of C. elegans, required for transposon silencing and RNA interference, is a homolog of Werner syndrome helicase and RNaseD. *Cell*, **99**, 133–141.